

Two-channel inhomogeneous TASEP with LK: A model of traffic flow

*Thesis submitted in partial fulfillment of the requirements for the award of the
degree of*

Master of Science

in

Mathematics and Computing

submitted by

Palak Chawla

(Reg no: 301503017)

Under Supervision of

Dr. Isha Dhiman



School of Mathematics
Thapar University
Patiala-147004, Punjab, India
July 2017

Certificate

I hereby certify that the work, which is being presented in the thesis, titled **Two-channel inhomogeneous TASEP with LK: A model of traffic flow**, in partial fulfillment of the requirements for the award of the degree of **Master of Science** in Mathematics and Computing, and submitted to Thapar University is an authentic record of my own work carried out under the supervision of **Dr. Isha Dhiman** . I have also cited the reference about the text(s)/figure(s) from where they have been taken.

The matter presented in this thesis has not been submitted elsewhere for the award of any other degree or diploma from any institution.



Palak Chawla

This is to certify that the above statement made by the candidate is correct to the best of our knowledge.



(Dr. Isha Dhiman)

Lecturer

School of Mathematics

Thapar University, Patiala

Abstract

In recent years, the application of statistical mechanics to non-equilibrium systems has become a major research area. Asymmetric simple exclusion process (ASEP) plays an important role in non-equilibrium mechanics. This thesis focuses mainly on the dynamics of an asymmetrically coupled two-channel totally asymmetric simple exclusion process with Langmuir Kinetics in presence of a localized bottleneck in any one of the lanes. This model is suitable to study real world situations occurring on multi-lane highways when the flow in one of the lanes is disturbed due to an accident or on some ongoing construction work

We have adopted the hybrid-approach along with the numerical scheme to obtain steady-state phase diagrams and density profiles. We have explored the consequences of different parameters such as bottleneck strength, coupling strength and size of the system on the steady-state dynamics. It is observed that on varying the bottleneck transition rates the topology of the phase diagrams is influenced. Also, an increase in the order of coupling strength reduces the bottleneck effect. Our theoretical arguments are in well agreement with extensively performed Monte-Carlo simulations.

Keywords: Langmuir Kinetics, Monte-Carlo simulations, bottleneck, phase diagrams, traffic-flow, two-channel.

Acknowledgements

First, I would like to express my deep gratitude towards my supervisor **Dr. Isha Dhiman**, School of Mathematics, Thapar University, Patiala, for her invaluable guidance, constant help and encouragement. Her broad knowledge and patience inspired me to face many challenges throughout the course of this work.

I would like to acknowledge **Dr. A.K. Lal**, Head, School of Mathematics, Thapar University for setting good standards for his students and providing all the help and facilities that were essential throughout the journey. His encouragement time and again has helped students to achieve the set goals. He has always been supportive and provided us required information at regular intervals.

I will be failing in my duty if I do not express my gratitude towards **Dr. S.S. Bhattia**, Dean of Academic Affairs, Thapar University for making provisions of infrastructure such as library facilities, computer labs equipped with Internet facilities, immensely useful for the learners to equip themselves with the latest knowledge in the field.

Above all, thanks to the Almighty, my family and friends for always being there for me and staying calm at times required.

Palak Chawla

Table of Contents

Abstract	ii
Table of Contents	iv
List of Figures	vi
Chapter 1 Introduction	1
1.1 Why do we need mathematical modeling?	1
1.1.1 Mathematical Modeling and the Scientific Method	1
1.1.2 Types of models	2
1.2 Asymmetric simple exclusion process(ASEP)	3
1.2.1 Types of update rules	4
1.2.2 Monte-Carlo simulations	5
1.2.3 Steady-state solutions of one-dimensional TASEP	6
1.3 Generalizations of ASEP	7
1.3.1 Multi-channel ASEP	7
1.3.2 Langmuir kinetics	8
1.3.3 Existence of inhomogeneity	8
1.4 Literature	9
1.5 Aims and Objectives	10
1.6 Outline of the thesis	11
Chapter 2 Two-channel inhomogeneous TASEP with LK under partial asymmetric coupling	12
2.1 Model and dynamical rules	12
2.2 Methodology	14
2.2.1 Theoretical Approach: Hybrid mean field(HMF)	14
2.2.2 Numerical Scheme	16
2.2.3 Monte-Carlo Simulations	17
2.3 Results and discussions	18
2.3.1 Impact of bottleneck strength	18
2.3.2 Impact of coupling strength	25
2.3.3 Impact of system size	28
2.4 Summary	28

Chapter 3	Conclusions and Future Works	29
3.1	Conclusion	29
3.2	Scope for future work	30
References		31

List of Figures

1.1	ASEP in one-dimensional lattice	4
1.2	The phase diagram representing different phases of ASEP	6
1.3	Schematic diagram of one-dimensional TASEP with LK	8
2.1	Schematic picture of two-channel inhomogeneous TASEP with LK .	13
2.2	Phase diagram for $\Omega_d = \Omega_a = 0.2$, $\Omega_A = 0.6$, $\Omega_B = 0.3$, $L=1000$, (a) $q=0.75$ (weak bottleneck), Notations:- 1:(S_b -S,LD/HD), 2:(LD-S,S/HD), 3:(S-HD,HD/HD), (b) $q=0.25$ (strong bottleneck), Notations:- 1:(LD-LD,LD/S), 2:(S_b -LD,LD/S), 3:(S_b -LD/HD/LD/HD), 4:(S_b -S,LD/HD/LD/HD), 5:(S_b -LD,HD/LD/HD), 6:(S_b -S,HD/LD/HD), 7:(S-HD,HD/HD), (c) $q=0$ (complete blockage), Notations:- 1: (S-LD,LD/S), 2:S-(LD,S/ S_b), 3:(HD-LD,S/ S_b), 4:(S_b -S,LD/S), 5:(S_b -S,S/HD), 6:(HD-S,S/HD)	20
2.3	Density profile for $q=0.25$, $\Omega_d=0.2$, $\Omega_A=0.6$, $\Omega_B=0.3$, $L=1000$, (a)(LD-LD,LD/LD) phase for $\alpha=0.05$, $\beta=0.6$, (b)(LD-S,LD/S) phase for $\alpha = 0.05$, $\beta = 0.1$ (c)(S_b -S,S/HD) phase for $\alpha=0.2$, $\beta=0.1$, (d)(S-HD,S/HD) for $\alpha=0.1$, $\beta=0.025$, (e)(HD-HD,HD/HD) phase for $\alpha=0.6$, $\beta=0.025$,(f)(HD-HD,HD/LD/HD) phase for $\alpha=0.75,\beta=0.4$, (g)(S_b -LD,LD/S) phase for $\alpha=0.2$, $\beta=0.38$	23
2.4	Conversion of spike into bottleneck induced shock with respect to an increase in α through (a)Continuum mean-field(CMF) and (b) Monte-Carlo simulations. Here, $q=0.25$, $\beta=0.1$, $L=1000$	25
2.5	Phase diagram for $\Omega_d =0.2$, $L=1000$ with (a) $q=0.25$, $\Omega_A =60$, $\Omega_B =30$. (b) $q=0.25$, $\Omega_A =600$, $\Omega_B =300$, Notations:- 1:(S_b -S,HD/LD/HD), 2:(S_b -S,S/HD), 3:(HD-S,HD/HD)	26
2.6	Variation in density profiles in lane A with respect to the order of lane-changing rates. Here, $\alpha=0.3$, $\beta=0.3$, $q=0.25$, (a)from CMF (b)from MCS	27
2.7	Variation in density profiles in lane A on changing the system size. Here, $\alpha=0.5$, $\beta=0.2$, $q=0.25$	28

Chapter 1

Introduction

A mathematical model is a description of a system using mathematical concepts and language i.e., it is a simplified representation in mathematical terms of the behavior of real world phenomena. It aims to describe the different aspects of the real world, their interaction and their dynamics through mathematics. It can be done through either equation or by computer code and are intended to mimic essential features while leaving out inessentials. Mathematical models are characterized by assumptions about:

- Variables (the things which change)
- Parameters (the things which do not change)
- Functional forms (the relationship between the two)

1.1 Why do we need mathematical modeling?

Since the modeling of devices and phenomena is essential to both engineering and science, engineers, and scientists have very practical reasons for doing mathematical modeling. In addition, engineers, scientists, and mathematicians want to experience the sheer joy of formulating and solving mathematical problems.

1.1.1 Mathematical Modeling and the Scientific Method

In an elementary picture of the scientific method, we identify a real world and a conceptual world. The external world is the one we call real; here we observe various phenomena and behaviors, whether natural in origin or produced by artifacts. The conceptual world is the world of the mind where we live when we try to understand what is going on in that real, external world. The conceptual world can be viewed as having three stages: observation, modeling, and prediction. In the observation part of the scientific method, we measure what is happening in the real world. Here we gather empirical evidence and facts on the ground. Observations may be direct, as when we use our senses, or indirect, in which case some

measurements are taken to indicate through some other reading that an event has taken place. For example, we often know a chemical reaction has taken place only by measuring the product of that reaction.

1.1.2 Types of models

Several classification criteria can be used for mathematical models according to their structure. Some of them are described as follows.

- **Linear vs. nonlinear:** If all the operators in a mathematical model exhibit linearity, the resulting mathematical model is defined as linear. A model is considered to be nonlinear otherwise. Linear models describe a continuous response variable as a function of one or more predictor variables.
- **Static vs. dynamic:** A dynamic model accounts for time-dependent changes in the state of the system, while a static (or steady-state) model calculates the system in equilibrium, and thus is time-invariant. Dynamic models typically are represented by differential equations.
- **Explicit vs. implicit:** If all of the input parameters of the overall model are known, and the output parameters can be calculated by a finite series of computations the model is said to be explicit. But sometimes it is the output parameters which are known, and the corresponding inputs must be solved for by an iterative procedure, such as Newton's method.
- **Discrete vs. continuous:** A discrete model treats objects as discrete, such as the particles in a molecular model or the states in a statistical model; while a continuous model represents the objects in a continuous manner, such as the velocity field of fluid in pipe flows, temperatures and stresses in a solid, and electric field that applies continuously over the entire model due to a point charge.
- **Deterministic vs. probabilistic (stochastic):** A deterministic model is one in which every set of variable states is uniquely determined by parameters in the model and by sets of previous states of these variables. Therefore, a deterministic model always performs the same way for a given set of initial conditions. For example, an amount of fluid a pipe can hold before breaking. Conversely, in a stochastic model usually called a statistical model randomness is present, and variable states are not described by unique values, but rather by probability distributions. Weather forecasting, rolling of dice are

examples of a stochastic model.

- **Deductive, inductive, or floating:** A deductive model is a logical structure based on a theory. An inductive model arises from empirical findings and generalization from them. The floating model rests on neither theory nor observation but is merely the invocation of expected structure.

1.2 Asymmetric simple exclusion process(ASEP)

This thesis is based on employing a discrete lattice gas model namely ASEP, which is of fundamental importance to non-equilibrium statistical mechanics. Statistical mechanics is the branch of theoretical physics, which uses probability theory to study the average behavior of a mechanical system, where the state of the system is uncertain. Non-equilibrium statistical mechanics deals with the issue of microscopically modeling the speed of irrevocable processes that are induced by imbalances. The characteristic feature of a non-equilibrium system is the existence of a nonzero particle current in its steady-state, which causes the particles to flow preferentially in a particular direction and hence, the name driven diffusive systems (DDS) follows.

Asymmetric simple exclusion process(ASEP) plays a crucial role in non-equilibrium mechanics. This is a stochastic model for describing the dynamics of interacting particles hopping right and left with different rates on a one-dimensional lattice with open boundaries. An exclusion principle allows this motion only when the target site is vacant. Exclusion processes refer to a collection of models of transport where particles have hard-core interaction. These models can be studied under different boundary conditions and different transition rates.

Fig.(1.1) shows the ASEP in one-dimensional lattice. If the site is empty at the first site particle will enter with a probability α and exit with probability β if last site is occupied. On a 1-D channel particles move forward with rate p and backwards with rate q . When $q = 0$ i.e., motion is in one direction only, it is totally asymmetric simple exclusion process(TASEP)[1, 2]. A particle hopping model conserves the total number of particles, at least in the bulk.

The first ASEP model was given by MacDonald [1] almost forty years ago summarizing the kinetics of bio-polymerization. During all these years ASEPs have been further applied to other processes, like, the movement of motor proteins along cytoskeleton filaments [3, 4], repton models of diffusion of polymer chains[1, 5], motion in ant trails [2] and car traffic [6].

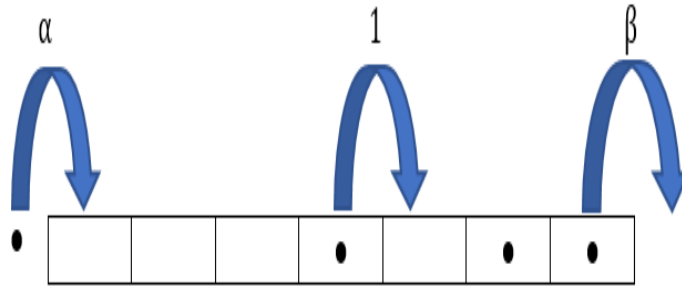


Figure 1.1: ASEP in one-dimensional lattice

1.2.1 Types of update rules

Simple one-channel exclusion processes model can be modified to incorporate details about certain traffic situations. For instance, a system can have more than one exit and entrance sites, it can have different transition rates for moving forward and backward, etc. So, the dynamics of the model is highly influenced by the type of update rules. There are four basic update rules [7].

1. *Random-sequential update rule:* We pick at random a site i . If $2 < i < L - 1$, each particle has a certain probability p of jumping to the right (if this site is empty). If $i = 1$ and entrance site is occupied then we allow for hopping to the right with probability p and particle injection with rate α if this site is empty. For $i = L$, a particle is removed with rate β if the site is occupied. This update is the realization of the usual master equation in continuous time. A different p would simply result in a rescaling of time. As a consequence, the phase diagram of the ASEP with this update depends only trivially on p . Therefore one can set $p=1$ which is most efficient for computer simulations. In this type the state of only one site is updated at each moment of time.

The following three updates are discrete in time.

2. *Sublattice-parallel update:* We first use our rule for injection(removal) at site $1(L)$ and also perform our rules for hopping on the pairs $(2,3)$, $(4,5)$ etc. After that, we update the pairs $(1,2)$, $(3,4)$ etc. (L has to be even). This

update can be used efficiently for computer simulations. It's main advantage for theoretical purposes is that its transfer matrix can be written as a product of local terms.

3. *Ordered-sequential update*: We start at the right end of the chain and remove a particle at site $i = L$ with probability β . We then update the pair $(i = L - 1, i = L)$. We continue with pair $(i = L - 2, i = L - 1)$ and so forth, until the left end of the chain is reached. After the update of pair $(i = 1, i = 2)$, we allow for injection at site $i = 1$. For models where particles only hop to the right this update may also be called more precisely "backward-ordered-sequential update."

Obviously, the order of update can also be reversed. For the ASEP, these two updates are connected by a particle-hole symmetry, injecting particles can be regarded as removing holes, and vice versa. Thus, it is sufficient to study just one of the ordered-sequential updates.

4. *Parallel update*: The rules for hopping, injection, and removal are applied simultaneously to all sites of the whole chain. The parallel update usually produces the strongest correlations and is used for traffic simulations. In the case of the ASEP, it is nearly identical to the particle-ordered-sequential update.

1.2.2 Monte-Carlo simulations

Monte-Carlo simulations is named after the casino in Monte-Carlo(MC), Monaco which is famous for gambling. Because the simulation technique involves generating chance variables and exhibits random behaviours, it has been called Monte-Carlo simulations(MCS). MC method was invented by Stanislaw Ulam in 1946 while pondering the probabilities of winning a card game. This technique is a common name for a wide variety of stochastic processes. These processes are based on sampling i.e, use of random numbers, and probability statistics to examine problems in various fields such as economics, statistical physics, bio-physics, flow of traffic and many more. This is basically adopted when there are too many particles in the system or when it is difficult to solve analytically or have complex interactions among the particles. MCS is a strong statistical analysis tool and widely used. This performs random sampling and conducts a large number of experiments on computer. The statistical traits of the experiments are observed and conclusions are drawn based on those simulations. We adopt Monte-Carlo simulations to analyze steady-state density profiles and phase diagrams of the ASEP

models.

1.2.3 Steady-state solutions of one-dimensional TASEP

The ASEP model is best comprehended for the steady-state solution. This is the position when a state of the system does not change with time. The steady-state solution in one-channel ASEP was given by Derrida [8] in 1998 using mean-field theory. We consider the random sequential update rules in which a random site is chosen. We will be concerned with mainly TASEP in which rate of movement to the left is 0 and right is 1. There are various interesting boundary induced phases of the ASEP in 1-D channel. Boundary induced phase transition is an important feature of non-equilibrium systems [9]. We obtain these phases by analyzing the density profiles of particles. Consider a 1-D lattice of length L . Steady-state consists of three phases depending on values of α and β as shown in Fig.(1.2).

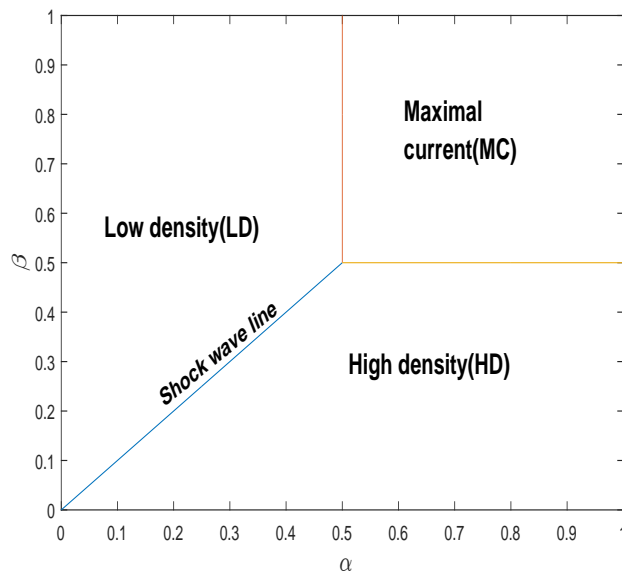


Figure 1.2: The phase diagram representing different phases of ASEP

- **Low-density(LD):** When $\alpha < \beta$ probability of entering a particle is less than the probability of leaving so more of the particles are leaving which implies system is in low density phase(LD). Mathematically, it is denoted by $\rho < \frac{1}{2}$ where ρ represents the density. Hence, this phase is entrance

dominated. The flow is given by $\alpha(1 - \alpha)$. As the entry rate increases density also increases from 0 to $\frac{1}{2}$ and it is given by $\rho = \alpha$.

- **High-density(HD):** When $\alpha > \beta$ more particles are entering to the system it is in high density phase which is denoted by $\rho > \frac{1}{2}$, mathematically. Traffic flow is a function of the exit rate only so this is exit dominated phase. The flow is computed by $\beta(1 - \beta)$. As the exit rate increases density decreases from 1 to $\frac{1}{2}$ and is given by $\rho=1-\beta$.
- **Maximal-current(MC):** When $\rho=\frac{1}{2}$ ($\alpha, \beta \geq \frac{1}{2}$) there is a balance in entering and leaving of particles so this phase is known as maximal current situation. Largest possible smooth flow of vehicles is achieved in this case. Moreover, the flow doesn't depend on the entry or exit rates. This flow is constant and is equal to $\frac{1}{4}$. Note that density is not the maximum in this phase even though the flow is maximum.
- **Shock-wave line:** Interestingly, when $\alpha = \beta < \frac{1}{2}$ there is a shock front on the road. This indicates a sudden shift from low to high density.

1.3 Generalizations of ASEP

1.3.1 Multi-channel ASEP

There are many real processes such as macroscopic clustering phenomena, traffic flow, motor protein dynamics and various systems of oppositely moving particles which comprise particles in motion in more than one channel. Thus, in order to comprehend the dynamical aspects of many-particle systems more appropriately, it is important to explore multi-channel ASEPs. In recent years, several investigations have been carried out on multi-channel ASEPs. Pronina and Kolomeisky established vertical cluster mean-field theory to study the effect of coupling strength between two channels. In TASEP two-channel model, the possible existence of seven distinct steady-state phases has been shown in the case when lane changing is completely biased in one direction. Tsekouras and Kolomeisky examined the role of coupling rates in a coupled TASEP and symmetric simple exclusion process(SSEP). In addition to this, various other aspects such as symmetry breaking, coexistence of phase, separation of phase with bidirectional transport and shock formation have been investigated in multi-channel ASEP models [10, 11, 12, 13].

1.3.2 Langmuir kinetics

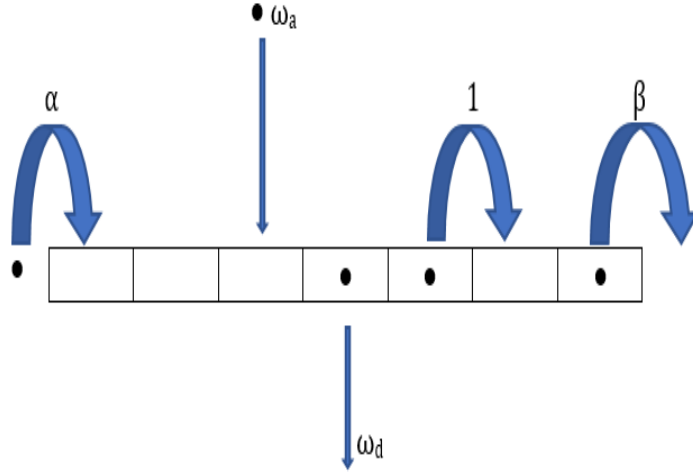


Figure 1.3: Schematic diagram of one-dimensional TASEP with LK

An important feature which is not taken into account by the TASEP is the notion of Langmuir Kinetics. We already know that in TASEP total number of particles are conserved in the system but particles can be attached or detached from the bulk which violates the phenomena of conservation of mass. For example, in real world, while travelling on a road or highway any vehicle can join the main highway from an on-ramp(attachment) and also it can move down the main highway by an off-ramp(dettachment). This attachment and detachment dynamics are known as **Langmuir Kinetics(LK)**. This feature has been included in a TASEP model by Parmeggiani et al. [14] in 2004. The incorporation of Langmuir Kinetics also performs significant transitions in phase diagrams. The TASEP with LK model dynamics have been explored in one-dimensional [14, 15] as well as two-dimensional [16, 17, 18, 19] models in literature. Fig.(1.3) shows the schematic diagram of one-dimensional TASEP with LK.

1.3.3 Existence of inhomogeneity

Suppose at any part of the highway, motion is obstructed by an ongoing construction or accident, etc. then the flow is reduced due to this obstruction. The notion of reducing the flow of vehicles at some defected sites can be considered as a set of inhomogeneous lattice sites i.e., bottleneck sites. This type of disorder is known

as site-wise disorder. Apart from this there is another inhomogeneity in the system which occurs when a vehicle is moving very slow (particle-wise disorder). In particle-wise disorder vehicle itself acts as an inhomogeneity in the system. In this thesis, we are focusing on the site-wise disorder in.

1.4 Literature

There is a lot of work already done on both single as well as multi-channel homogeneous TASEPs as discussed till the previous section. But the steady-state dynamics of inhomogeneous systems is not well understood. Single-channel inhomogeneous TASEP with [20] and without LK [5, 21, 22, 23, 24, 25] has been diversely studied. While exploring the characteristics and effects of a bottleneck in a closed TASEP, it was observed that the existence of even a single bottleneck site can develop shock profile and a plateau in the fundamental current-density relation. Kolomeisky [25] further investigated a higher model of single-channel open system and reviewed the consequences of the inhomogeneity with both slow and fast transition rates. He parted the system into two homogeneous TASEPs with a single bottleneck site (*defect mean-field theory* (DMFT)) and concluded that a fast site has no effect on the steady-state phase diagram; while a slow site leads to shifting of the phase boundaries only. He also verified the theoretical results with Monte Carlo simulations and noted a good agreement in low-density (LD) and high-density (HD) phase whereas a small variation was found in maximal current (MC) phase. In addition to this approach, Chou and Lakatos [5] introduced another analytical approach namely *finite-segment mean-field theory* (FSMFT). Their study focused on the clusters of slow codons in protein synthesis. They detected that ribosome density profiles in the neighbourhood clusters of slow codons suppress the protein synthesis. A generalization of DMFT was made by Dong et al [21]. to analyze the impact of two bottlenecks in the protein production rate and also executed large-scale Monte Carlo simulations. He concluded that the site as well as distance between the bottlenecks have an effect on the production rate and identified an important phenomenon namely *edge effect*. The study of edge effects was later proceeded by Greulich and Schadschneider [22] to develop the phase diagrams of inhomogeneous TASEP using *interacting subsystem approximation* (ISA). They describe the interactions of defects with the boundaries of the single-channel system. Moreover, Qiu et al. [26] explained more complex case of inhomogeneous TASEP with LK. They determined phase diagrams and density

profiles using the DMFT approach and also analyzed the consequences of slow hopping and detachment rate of phase diagram. The investigation was further carried out by Pierobon et al. [20]. They presented a detailed study on the role of bottleneck in a TASEP with LK, by adopting mean-field theory and Monte Carlo simulations. The idea of carrying capacity to point out different novel phases known as bottleneck phases was also established by them. Note that all of the above studies emphasized on single-lane inhomogeneous systems.

In the same way as of single-channel system, particles in multi-channel transport system [10, 16, 17, 27] may also experience an obstacle present in either one or more than one lanes. It is difficult to study the consequences of inhomogeneity in multi-channel open system due to the complexity in dynamics by various interactions between different channels. Wang et al. [28] contributed a lot in this direction. They examined the effects of a local inhomogeneity in one of the lane of a two-channel TASEP with LK under symmetric coupling. They expanded the DMFT to a two-channel system by including the notion of effective entrance and exit rates at the inhomogeneous lattice site. Further Dhiman and Gupta [29] highlighted the limitation of DMFT approach. They found that although solution of the mean-field equations supported Monte Carlo simulations in ref. [28], but DMFT was unsuccessful to generate the steady-state phase diagram of two-lane inhomogeneous system. Besides, it is not feasible to study the effects of different parameters like lane-changing rate, strength of bottleneck, attachment-detachment rates on the steady-state dynamics. Thus, we can say that DMFT, inspite of providing analytic solutions for single-channel inhomogeneous TASEPs with and without LK, fails to describe some significant components to produce an entire picture of the dynamics of the corresponding two-channel system. So a new approach known as *hybrid mean-field approach* was introduced by Dhiman and Gupta in ref. [29] to analyze the bottleneck in a two-channel symmetrically coupled TASEP with LK.

1.5 Aims and Objectives

The aim of this thesis is to study the two-channel TASEP with LK in the presence of a single localized inhomogeneity (bottleneck) in one of the two lanes. The model is analyzed under partially asymmetric coupling conditions. It is to be noted that so far the inhomogeneous two-channel model has not been studied under partially asymmetric coupling conditions, which motivates us to take up this problem and

study in this thesis. The specific objectives of this thesis are:

- to investigate the stationary-behaviour of two-channel system under the effect of a static bottleneck.
- to examine the thorough effect of bottleneck strength on system dynamics.
- to explore the effects of lane-changing rates and its interactions with the bottleneck.
- to analyze the effect of system size and to identify the finite-size effects, if any.

1.6 Outline of the thesis

Chapter-1 provides a brief review to the general aspects of mathematical modeling and different types of models. Specifically, a discrete model namely asymmetric simple exclusion process(ASEP) is discussed. In this chapter the objectives of this thesis along with a survey of the literature are presented.

Chapter-2 provides the complete description of dynamics of the totally asymmetric simple exclusion process(TASEP) with Langmuir Kinetics(LK) having a single localized inhomogeneity. We thoroughly study the role of various parameters on the steady-state dynamics of the system by means of phase diagrams and density profiles. Monte-Carlo simulations are carried out to validate theoretical results.

Chapter-3 summarizes the key outcomes of the work done along with the possible future research directions.

Chapter 2

Two-channel inhomogeneous TASEP with LK under partial asymmetric coupling

In this chapter, we introduce the two-channel TASEP model with LK in the presence of a single localized bottleneck site in one of the lanes. The model is studied under partially asymmetric coupling conditions under which the lane-changing rates of particles from one lane to another are unequal (both non-zero).

The chapter is organized as follows. In section 2.1, we define the model and its dynamical rules. The hybrid mean-field approach along with the numerical scheme are provided in section 2.2. Section 2.3 deals with the steady-state solution of the system and presents the phase diagrams computed by numerical scheme and then validated through Monte-Carlo simulations. A brief summary of the outcomes is provided in concluding section 2.4.

2.1 Model and dynamical rules

The model is defined in a two-channel lattice $(L, 2)$ (see fig. (2.1)) where L denotes the total number of sites or length of a channel. These channels are indicated by A and B in which particles follow hard-core exclusion principle. The system follows random sequential dynamics i.e., a site is chosen at random and at each time step the state of only one site is updated. A lattice site $(i, j); i = 1, 2, \dots, L; j = A, B$; is randomly chosen for each time step. The state of each site is characterized by an occupation number $\eta_{i,j}$ defined as

$$\eta_{i,j} = \begin{cases} 1 ; & \text{if } i^{\text{th}} \text{ site is occupied} \\ 0 ; & \text{if } i^{\text{th}} \text{ site is vacant} \end{cases} \quad (2.1)$$

The configuration of the lattice is updated as per the following dynamical rules.

- Entrance site ($i = 1$): A particle enters the lattice with a probability α if $\eta_{1,j}=0$.

- Exit site($i = L$): A particle leaves the lattice with a probability β provided $\eta_{L,j}=1$.
- Bulk sites :
 1. If $\eta_{i,j}=1$,
 - the particle at site (i, j) first tries to detach itself from the system with rate ω_d .
 - If it doesn't succeeds it checks it's foward site and moves forward with a rate $p_{i,j}$ (see eq. (2.2)) if $\eta_{i+1,j}=0$.
 - Else it attempts to jump to the other lane only if the target site in other lane is vacant. Here ω_A and ω_B denotes the lane changing rates from lane A to B and B to A respectively.
 2. if $\eta_{i,j}=0$, a particle can attach to the system with rate ω_a .

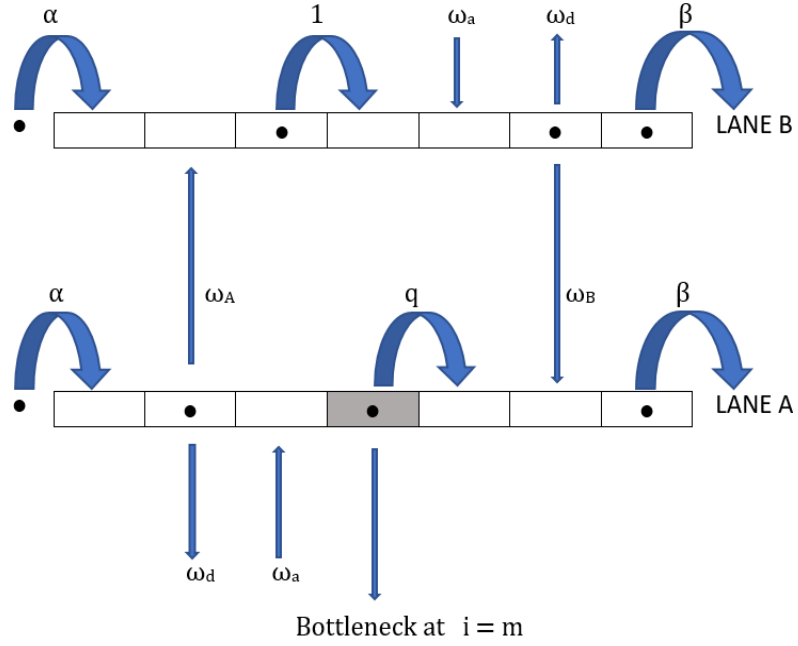


Figure 2.1: Schematic picture of two-channel inhomogeneous TASEP with LK

Consider the bottleneck site to be present in lane A , and at site ' m ' while homogeneity is kept in lane B . We further assume that $1 \ll m \ll L$.

$$p_{i,j} = \begin{cases} q ; & \text{if } i = m \text{ and } j = A \\ 1 ; & \text{else} \end{cases} \quad (2.2)$$

Here q is the bottleneck rate i.e., the transition rate of a particle on passing through the bottleneck site. Note that all the rates lie between the interval $[0,1]$. Although these dynamic rules are quite simple, they produce a very complex dynamic phase behaviour. On varying even one of the rates in the lattice our system may go from one regime to the other.

2.2 Methodology

2.2.1 Theoretical Approach: Hybrid mean field(HMF)

This is a theoretical approach in which instead of dividing both the lanes into sub-lanes, we divide the lane A (inhomogeneous lane) into two subsystems i.e., $1 \leq i < m$ and $m + 1 < i \leq L$ connected through the sites $i = m$ and $i = m + 1$. Firstly we figure out the transitory evolution of occupation probabilities $\eta_{i,j}$ in the bulk sites from the following set of master equations:

$$\begin{aligned} \frac{d\langle\eta_{i,j}\rangle}{dt} = & p_{i-1,j}\langle\eta_{i-1,j}(1-\eta_{i,j})\rangle - p_{i,j}\langle\eta_{i,j}(1-\eta_{i+1,j})\rangle - \omega_a\langle\eta_{i,j}\rangle + \omega_a\langle 1-\eta_{i,j}\rangle \\ & \mp (\omega_A(\langle\eta_{i,A}\eta_{i+1,A}(1-\eta_{i,B})\rangle) - \omega_B(\langle\eta_{i,B}\eta_{i+1,B}(1-\eta_{i,A})\rangle)) \end{aligned} \quad (2.3)$$

where $\langle\dots\rangle$ denotes the statistical average and the last term takes negative and positive signs for $j = A$ and $j = B$ respectively. At the boundaries, the particle densities evolve in accordance with

$$\frac{d\langle\eta_{1,j}\rangle}{dt} = \alpha\langle 1-\eta_{1,j}\rangle - p_{1,j}\langle\eta_{1,j}(1-\eta_{2,j})\rangle \quad (2.4)$$

$$\frac{d\langle\eta_{L,j}\rangle}{dt} = p_{L,j}\langle\eta_{L-1,j}(1-\eta_{L,j})\rangle - \beta\langle\eta_{L,j}\rangle \quad (2.5)$$

We can factorize the correlations as follows using mean field approximation,

$$\langle\eta_{i,j}\eta_{i+1,j}\rangle = \langle\eta_{i,j}\rangle\langle\eta_{i+1,j}\rangle$$

Hybrid continuum mean-field equations To find the continuum limit of the above equations, a lattice constant $\epsilon = 1/L$ is defined. All the parameters i.e.,

time and other transition rates are rescaled as $t' = t/L$, $\Omega_a = \omega_a L$, $\Omega_d = \omega_d$, $\Omega_A = \omega_A L$, $\Omega_B = \omega_B L$ [29].

Write $x = (i - 1)\epsilon$, replace binary discrete variables $\eta_{i,j}$ with continuous variables $\rho_{i,j} \in [0, 1]$ and retain the terms upto second order Taylor series expansion to get

$$\rho_{i\pm 1,j} = \rho_{i,j} \pm \epsilon \frac{\partial \rho_{i,j}}{\partial x} + \frac{\epsilon^2}{2} \frac{\partial^2 \rho_{i,j}}{\partial x^2} + O(\epsilon^3) \quad (2.6)$$

Lane B: As we know that lane B is free from any inhomogeneity, we can ignore the subscript i and compute the time evolution equation from master equations (2.3) and (2.6) for mean density in lane B , denoted by ρ_B .

$$\begin{aligned} \frac{\partial \rho_B}{\partial t'} &= \frac{\epsilon}{2} \frac{\partial^2 \rho_B}{\partial x^2} + \frac{\partial}{\partial x} (\rho_B^2 - \rho_B) + \Omega_d (K - (K + 1)\rho_B) \\ &\quad + \Omega_A (\rho_A^2 (1 - \rho_B) - \Omega_B (\rho_B^2 (1 - \rho_A))) \end{aligned} \quad (2.7)$$

where $K = \frac{\Omega_a}{\Omega_d}$ is the binding constant [14].

Lane A: Lane A is divided into two sub-lanes due to the presence of inhomogeneity viz., $1 < i < m$ and $m + 1 < i < L$ connected through sites $i = m$ and $i = m + 1$. The two subsystems of lane A are individually homogeneous TASEPs with LK, so we can compute the continuum limit of the master equation for each subsystem in lane A by proceeding same as lane B . We get the following hybrid system of equations for time evolution of mean density in lane A , denoted by ρ_A .

Continuum part: $x \in (0, m\epsilon) \cup ((m + 1)\epsilon, 1)$

$$\begin{aligned} \frac{\partial \rho_A}{\partial t'} &= \frac{\epsilon}{2} \frac{\partial^2 \rho_A}{\partial x^2} + \frac{\partial}{\partial x} (\rho_A^2 - \rho_A) + \Omega_d (K - (K + 1)\rho_A) \\ &\quad - \Omega_A (\rho_A^2 (1 - \rho_B) + \Omega_B (\rho_B^2 (1 - \rho_A))) \end{aligned} \quad (2.8)$$

The densities at $i = m$ and $i = m + 1$ in lane A , is computed by :

$$\begin{aligned} \frac{\partial_{m,A}}{\partial t'} &= \frac{1}{\epsilon} \rho_{m-1,A} (1 - \rho_{m,A}) - \frac{q}{\epsilon} \rho_{m,A} (1 - \rho_{m+1,A}) + \Omega_d (K - (K + 1)\rho_{m,A}) \\ &\quad - \Omega_A (\rho_{m,A} \rho_{m+1,A} (1 - \rho_{m,B}) + \Omega_B (\rho_{m,B} \rho_{m+1,B} (1 - \rho_{m,A}))) \end{aligned} \quad (2.9)$$

$$\begin{aligned}
\frac{\partial_{m+1,A}}{\partial t'} &= \frac{q}{\epsilon} \rho_{m,A} (1 - \rho_{m+1,A}) - \frac{1}{\epsilon} \rho_{m+1,A} (1 - \rho_{m+2,A}) + \Omega_d (K - (K+1) \rho_{m+1,A}) \\
&\quad - \Omega_A (\rho_{m+1,A} \rho_{m+2,A} (1 - \rho_{m+1,B}) + \Omega_B (\rho_{m+1,B} \rho_{m+2,B} (1 - \rho_{m+1,A}))
\end{aligned} \tag{2.10}$$

The boundary equations (2.4) and (2.5) reduce to $\rho_A(0) = \rho_B(0) = \alpha$ and $\rho_A(1) = \rho_B(1) = 1 - \beta$. As well, no approximation other than mean-field theory has been used to develop the hybrid system for a two-lane inhomogeneous TASEP with LK. It is clear that this hybrid approach only divides the inhomogeneous lane into sub-lanes without disturbing the homogeneous one. This notion makes it applicable to more general systems like multi-channel or those with more than one bottleneck sites.

We combine the equations (2.7),(2.8),(2.9) and (2.10) into a single system(see eq. (2.11)) by introducing another space variable x' where $0 < x' < m\epsilon$, $(m+1)\epsilon < x' < 1$ and $0 < x < 1$.

$$\begin{aligned}
\frac{\epsilon}{2} \frac{d^2 \rho_A}{dx'^2} + (2\rho_A - 1) \frac{d\rho_A}{dx'} + \Omega_d (K - (K+1)\rho_A) - \Omega_A \rho_A^2 (1 - \rho_B) + \Omega_B \rho_B^2 (1 - \rho_A) &= 0, \\
\rho_{m-1,A} (1 - \rho_{m,A}) - q \rho_{m,A} (1 - \rho_{m+1,A}) + \omega_d (K - (K+1)\rho_{m,A}) \\
&\quad - \omega_A \rho_{m,A} \rho_{m+1,A} (1 - \rho_{m,B}) + \omega_B \rho_{m,B} \rho_{m+1,B} (1 - \rho_{m,A}) = 0, \\
q \rho_{m,A} (1 - \rho_{m+1,A}) - q \rho_{m+1,A} (1 - \rho_{m+2,A}) + \omega_d (K - (K+1)\rho_{m+1,A}) \\
&\quad - \omega_A \rho_{m+1,A} \rho_{m+2,A} (1 - \rho_{m+1,B}) + \omega_B \rho_{m+1,B} \rho_{m+2,B} (1 - \rho_{m+1,A}) = 0, \\
\frac{\epsilon}{2} \frac{d^2 \rho_B}{dx^2} + (2\rho_B - 1) \frac{d\rho_B}{dx} + \Omega_d (K - (K+1)\rho_B) + \Omega_A \rho_A^2 (1 - \rho_B) - \Omega_B \rho_B^2 (1 - \rho_A) &= 0.
\end{aligned} \tag{2.11}$$

2.2.2 Numerical Scheme

Solving this system analytically is quite cumbersome because of its hybrid nature so we use numerical finite difference technique to find the steady-state solution of the hybrid system. This technique has been well defined for exploring two-channel homogeneous TASEP with LK [16, 17].

We project a generalized methodology to find the solution of the hybrid system. Instead of solving it explicitly, we find the steady-state solution by taking the long time solution of (2.7),(2.8),(2.9) and (2.10) using the following scheme [16, 17].

By using center difference formula for first order and second order space derivatives

and forward difference for time derivatives in equations (2.7),(2.8),(2.9) and (2.10), with the boundary conditions, $\rho_A(0)=\rho_B(0)=\alpha$ and $\rho_A(1)=\rho_B(1)=1-\beta$, we get the following difference equations for $1 < i < m$, $m + 1 < i < L$ with $j=A$ and $1 < i < L$ with $j=B$.

$$\begin{aligned} \rho_{i,j}^{n+1} = & \rho_{i,j}^n + \frac{\epsilon}{2} \frac{\Delta t'}{\Delta x^2} \left(\rho_{i+1,j}^n - 2\rho_{i,j}^n + \rho_{i-1,j}^n \right) + \frac{\Delta t'}{2\Delta x} \left((2\rho_{i,j}^n - 1)(\rho_{i+1,j}^n - \rho_{i-1,j}^n) \right) \\ & + \Delta t' \left[\Omega_d(K - (K + 1)\rho_{i,j}^n) \mp \left(\Omega_A(\rho_{i,A}^n)^2(1 - \rho_{i,B}^n) - \Omega_B(\rho_{i,B}^n)^2(1 - \rho_{i,A}^n) \right) \right] \end{aligned} \quad (2.12)$$

$$\begin{aligned} \rho_{m,A}^{n+1} = & \rho_{m,A}^n + \Delta t' \left[\frac{1}{\epsilon} \rho_{m-1,A}^n (1 - \rho_{m,A}^n) - \frac{q}{\epsilon} \rho_{m,A}^n (1 - \rho_{m+1,A}^n) + \Omega_d(K - (K + 1)\rho_{m,A}^n) \right. \\ & \left. - \Omega_A \rho_{m,A}^n \rho_{m+1,A}^n (1 - \rho_{m,B}^n) + \Omega_B \rho_{m,B}^n \rho_{m+1,B}^n (1 - \rho_{m,A}^n) \right] \end{aligned} \quad (2.13)$$

$$\begin{aligned} \rho_{m+1,A}^{n+1} = & \rho_{m+1,A}^n + \Delta t' \left[\frac{q}{\epsilon} \rho_{m,A}^n (1 - \rho_{m+1,A}^n) - \frac{1}{\epsilon} \rho_{m+1,A}^n (1 - \rho_{m+2,A}^n) + \Omega_d(K - (K + 1)\rho_{m+1,A}^n) \right. \\ & \left. - \Omega_A \rho_{m+1,A}^n \rho_{m+2,A}^n (1 - \rho_{m+1,B}^n) + \Omega_B \rho_{m+1,B}^n \rho_{m+2,B}^n (1 - \rho_{m+1,A}^n) \right] \end{aligned} \quad (2.14)$$

2.2.3 Monte-Carlo Simulations

We use Monte-Carlo simulations(MCS) to simulate the two-channel for validation of the results obtained by the theoretical mean-field hybrid approach. Random-sequential dynamical rules are adopted, which is the apprehension of the usual master equations in continuous time. We run the Monte-Carlo simulations for $10^8 - 10^{11}$ time steps and ignore first 5% steps to ensure the occurrence of steady-state. To compute the densities in both the lanes, time averages over an interval of $10L$ have been taken. Since the size of a real system is usually not very large, so it is appropriate to simulate the system for a lattice size upto $L=1000$. Taking into account all the dynamical rules that include various kinds of hoppings like horizontal,vertical transitions,attachment and detachment dynamics, it is quite expensive to compute steady-state densities using MCS.

2.3 Results and discussions

In this section, a thorough analysis of the steady-state properties of the model is provided emphasizing on the resulting phase diagrams and effect of bottleneck, lane-changing rate on the system. A bottleneck can be a result of accidents, road works, road curves and decrease in number of road lanes, etc. The steady state phase diagrams and density profiles are obtained from the hybrid mean-field approach and validated by the means of Monte-Carlo simulations.

We've assumed that the bottleneck is located at the middle i.e., $m = \frac{L}{2}$. We use $L = 1000$, $\Delta x = \frac{1}{L} = 0.001$, $\Delta t = 0.0005$ for the computations by mean-field approach satisfying the stability condition for the numerical scheme discussed in the previous section $|\frac{\Delta t}{\Delta x}| \leq 1$. We consider the situation in which the bottleneck acts as a slow inadequacy i.e. $q < 1$. The attachment and detachment rates are fixed at $\Omega_a = \Omega_d = 0.2$ ($K=1$).

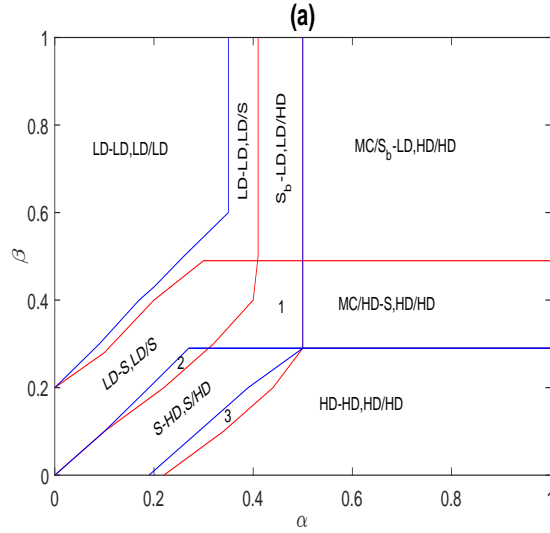
Notation $(Ph_{A(left)} - Ph_{A(right)}, Ph_B)$ indicates the kind of stationary phase in the two-channel lattice. In this, $Ph_{A(left)}$ ($Ph_{A(right)}$) depicts the type of steady-state phase in left(right) subsystem of lane A whereas Ph_B depicts the steady phase in lane B . Furthermore, density profiles can be of mixed type i.e, a part of it can lie in any one of the phases among LD(low-density), HD(high-density), MC(maximal current) or S(shock) whereas the rest part of lies in other phase. We call such profiles as mixed type and corresponding phases are known to be intermediate or coexistence phases. Slash(/) denotes the separation of phases in the same profile.

2.3.1 Impact of bottleneck strength

We explore the steady-state dynamics for different bottleneck strength by gradually decreasing the value of q from $q=1$ (homogeneity) to $q=0$ (complete blockage). Fig.(2.2) shows the phase diagrams of different bottleneck strength. When there is no blockage ($q=1$) then this model reduces to the homogeneous two-lane TASEP with LK which has been studied in detail in literature [16]. Note that, there are significantly less changes found in the phase diagram till $q \approx 0.75$ as the strength of the bottleneck is quite weak. On reducing the value of q below 0.75 one notices the considerable effect of bottleneck.

2.3.1.1 Phase diagrams

It is essential to study the phase diagrams thoroughly for better and intuitive understanding of the steady-state dynamics of the system. In case of symmetric coupling [29] in which particle jump from one lane to the other with equal rates, there is not a huge difference between phase diagrams of a weak bottleneck i.e., $q=0.75$ and no bottleneck ($q=1$). Although, the qualitative nature of some phases might differ but the topological structure is almost identical. As a matter of fact a weak bottleneck is unable to affect the steady-state dynamics in symmetric coupling. The prime effects can be seen in the congestion surrounded region. But because of the partially asymmetric coupling in which vehicles can hop to other lanes with unequal rates, there is a significant variation in the stationary-phase diagram in case of even weak bottleneck. Fig. 2.2(a) represents the phase diagrams of model $q = 0.74$ (weak bottleneck) with $\Omega_A = 0.6$ and $\Omega_B = 0.3$, which shows rich composition of steady-state phases.



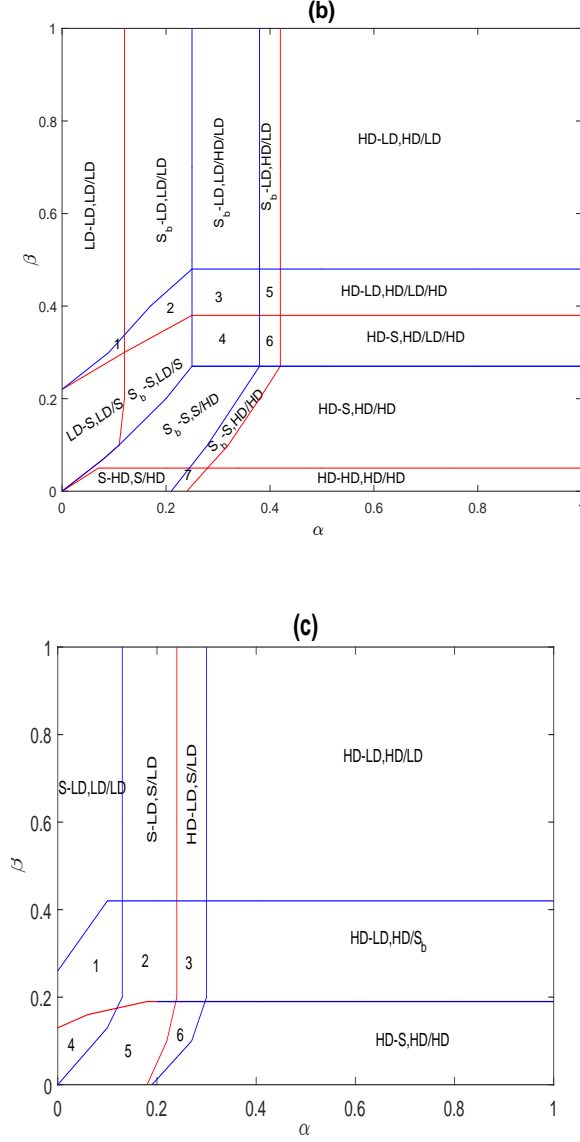


Figure 2.2: Phase diagram for $\Omega_d = \Omega_a = 0.2$, $\Omega_A = 0.6$, $\Omega_B = 0.3$, $L=1000$, (a) $q=0.75$ (weak bottleneck), Notations:- 1:(S_b -S,LD/HD), 2:(LD-S,S/HD), 3:(S-HD,HD/HD), (b) $q=0.25$ (strong bottleneck), Notations:- 1:(LD-LD,LD/S), 2:(S_b -LD,LD/S), 3:(S_b -LD/HD/LD/HD), 4:(S_b -S,LD/HD/LD/HD), 5:(S_b -LD,HD/LD/HD), 6:(S_b -S,HD/LD/HD), 7:(S-HD,HD/HD), (c) $q=0$ (complete blockage), Notations:- 1: (S-LD,LD/S), 2:S-(LD,S/ S_b), 3:(HD-LD,S/ S_b), 4:(S_b -S,LD/S), 5:(S_b -S,S/HD), 6:(HD-S,S/HD)

It can be seen that the bottleneck effect is observed in both the lanes due to asymmetric coupling rates. Particles tend to move into the other lane when the hopping rate of the inhomogeneous site is small. Observe that the number of steady-state phases in weak bottleneck is more than in case of homogeneous traffic system, which is due to the occurrence of mixed phases. The key distinguishing feature of the diagram is the appearance of bottleneck-induced shock which is the shock emerged due to the inhomogeneity only.

From the figure (2.2), it is clear that as we move from $q=0.75$ (weak bottleneck) to $q=0.25$ (strong bottleneck) the number of phases increases. We observe that there is no MC phase for $q=0.25$. The mixed phases (MC/HD-S,HD/HD), (MC/S_b-LD,HD/HD) existing for $q=0.75$ are replaced by (HD-LD,HD/LD/HD), (HD-LD,HD/LD). So the topology of the phase diagram is changed significantly. Besides, the bottleneck effect is sufficiently high to increase the density difference between two lanes due to which the complexity of phase diagrams also raises.

It is known that for a strong bottleneck, there is no LD phase in the left subsystem of lane A in case of symmetric coupled lanes but we find LD phase in the left subsystem of lane A , which occurs due to the partially asymmetric coupling. Since lane-changing rate from lane A to B is considerably higher than that of lane-changing rate from lane B to A , particles tend to move to the lane B more frequently contributing to the occurrence of LD phase in lane A . In comparison with $q=.75$ we find that there are more phases comprising of bottleneck-induced shock for $q=0.25$. The presence of shock or a HD phase in left subsystem($q=0.25$) is justified as the extremely slow transition rate at bottleneck site obstructs the incoming of particles. With the fall in the value of q , we can clearly see that (HD-LD,HD/LD) phase expands.

In the situation of complete blockage($q=0$), the presence of bottleneck-induced shock has been seen in lane B as well. In other words there is a significant impact of bottleneck in lane B also in this case. Further, there is no LD phase in left subsystem of lane A which is again due to complete obstruction by the bottleneck. Due to similar reasons there is no HD phase in right subsystem of lane A .

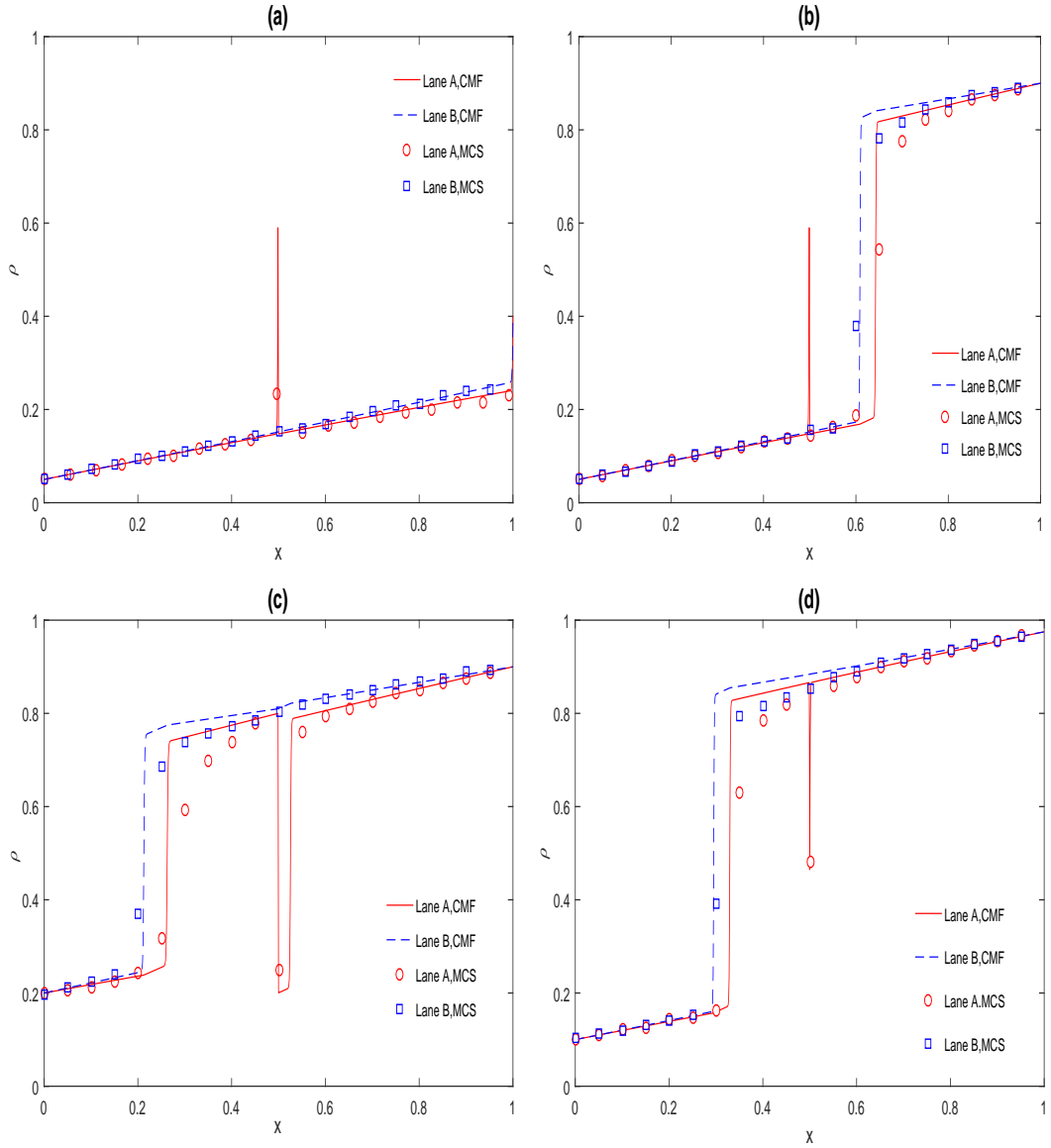
2.3.1.2 Density-profiles

Fig.(2.3) represents the density profiles for various steady-state phases with $q=0.25$. These have been obtained from the numerical solution of hybrid mean-field system and validated with MCS. We note that there is a good agreement between continuum mean-field(CMF) and Monte-Carlo simulations(MCS). We list some important features of the steady-state dynamics under the given choice of parameters.

1. *Phase transitions and intermediate phases:* On analyzing the phase transitions one observes the formation of shock through deconfinement of the

boundary layers.

Moreover, the bulk phase transition from (LD-LD,LD/LD) (fig.2.3(a)) to (LD-S,LD/S) (fig. 2.3(b)) can be interpreted by reducing β , the shock moves leftwards and reaches at $x=\frac{1}{2}$. This line is corresponding to the transition of phase between (LD-S,LD/S) and (S-HD,S/HD). A further decrease in β gives rise to (S-HD,S/HD) phase by moving the shock upstream to the bottleneck.



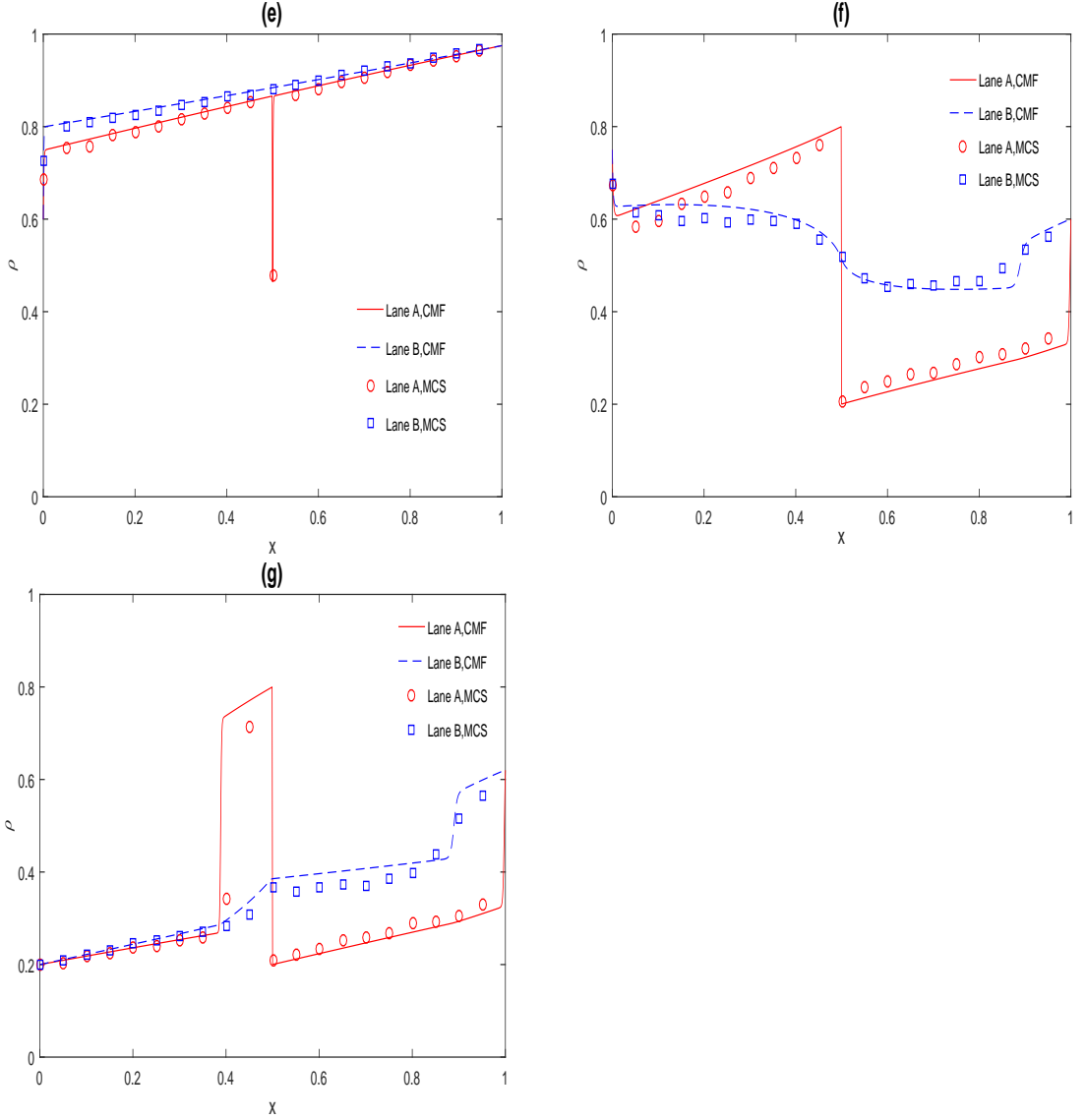


Figure 2.3: Density profile for $q=0.25, \Omega_d=0.2, \Omega_A=0.6, \Omega_B=0.3, L=1000$, (a)(LD-LD,LD/LD) phase for $\alpha=0.05, \beta=0.6$, (b)(LD-S,LD/S) phase for $\alpha=0.05, \beta=0.1$ (c) $(S_b-S,S/HD)$ phase for $\alpha=0.2, \beta=0.1$, (d)(S-HD,S/HD) for $\alpha=0.1, \beta=0.025$, (e)(HD-HD,HD/HD) phase for $\alpha=0.6, \beta=0.025$,(f)(HD-HD,HD/LD/HD) phase for $\alpha=0.75, \beta=0.4$, (g) $(S_b-LD,LD/S)$ phase for $\alpha=0.2, \beta=0.38$.

Note that, a shock is present in both the lanes in (S-HD,S/HD) shown in fig.2.3(d) for $\alpha=0.1, \beta=0.025$. On increasing α , the shock in both the lanes shifts towards left and converts to the phase (HD-HD,HD/HD) (fig.2.3(e)). The existence of other phase transitions in the phase diagram shown in fig.(2.2(b)) can be understood as a result of gradual changes in densities with respect to the boundary conditions. In fig (2.3)(a),(b),(c),(d),(e) the effect of bottleneck is only in vicinity of bottleneck but the effect of bottle-

neck is over a larger domain in figures fig. (2.3)(f) and (g). The difference is due to the variation in lane-changing rate and bottleneck rate which lead to peculiar kinds of density profiles.

2. *Emergence of upward and downward spikes:* We notice that the vehicles have enough space to move along the system in LD phase in left subsystem of lane A . When the vehicle reaches at bottleneck site it experiences a local congestion which results in the form of an upward spike in its density profile, as seen in fig.(2.3(a)). The vehicles coming from left feels a little obstacle before entering the bottleneck due to the smaller value of q . This results to the increase in density in lane A to a certain extent, just upstream to the bottleneck leading to the emergence of an upward spike in density profile. But lane B does not experiences such perturbation and remains unaffected in this phase. Now, consider the HD phase, where the vehicles are in a highly packed situation when these vehicles come out of the bottleneck through this high congestion they feel a sudden rise in its hopping rate leading to the emergence of a LD region just downstream to the bottleneck. This results in the formation of a downward spike as seen in fig (2.3)(d).

3. *Existence of a bottleneck-induced shock:* It is prior to know that formation of a bottleneck-induced shock (denoted by S_b) is one of the most significant feature of this system dynamics. Consider the LD phase in lane A , the number of vehicles in left subsystem of lane A increases with an increase in the entrance rate α . This results in the increase of existing upward spike to a certain height. At a specific $\alpha = \alpha_a = 0.2$, this local density disturbance(spike) converts into a shock. Fig. (2.4) shows the conversion of spike into bottleneck-induced shock with respect to an increase in entrance rate(α). Note that the height of upward spike in lane A at bottleneck site($x=\frac{1}{2}$) increases with the small rise in α . The spike gets converted into shock on increasing α and this bottleneck-induced shock shifts towards left as we further increase α . After the transition of spike into shock height of the shock remains the same even with a rise in the entrance rate. This leads to the transition of the spike into a shock. As this shock occurs due to bottleneck only, this is called bottleneck-induced shock. Note that there are a number of mixed/intermediate phases(fig. 2.2(b)) which are due to the existence of this bottleneck-induced shock. Moreover, in some cases we find the presence of S_b in lane B as well which indicates the effect of bottleneck in lane B too. In fig. (2.3(c)) there are two shocks in lane A , the left one

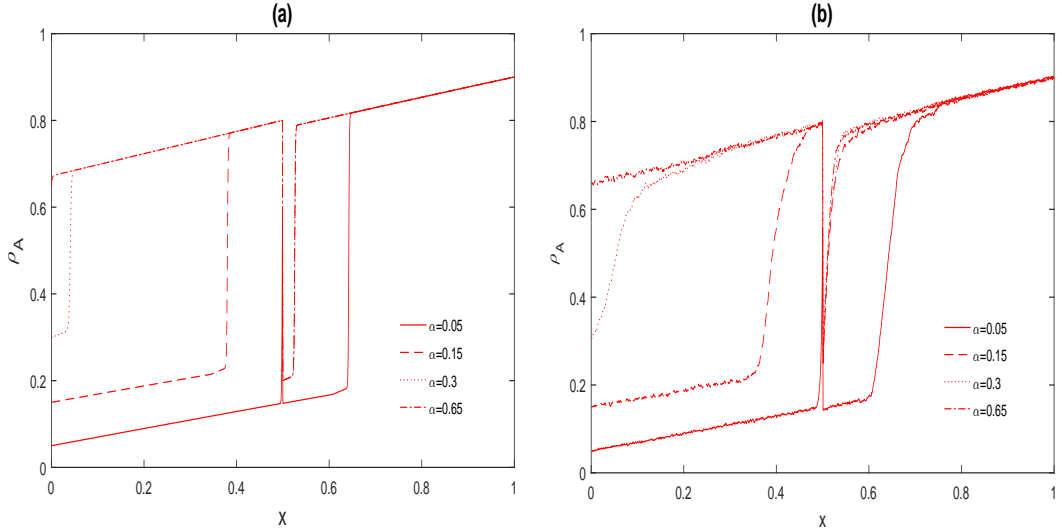


Figure 2.4: Conversion of spike into bottleneck induced shock with respect to an increase in α through (a) Continuum mean-field (CMF) and (b) Monte-Carlo simulations. Here, $q=0.25$, $\beta=0.1$, $L=1000$

being bottleneck-induced and the other one is due to the deconfinement of boundary layer.

2.3.2 Impact of coupling strength

Till now, we have discussed the system dynamics under various bottleneck strengths keeping the coupling-rate constant. As we know that lane-changing rate plays a crucial role in two-channel models, so it is important to analyze its effect on our system. It is well explained in literature [10, 16, 19], that higher order of lane-changing rate significantly affects the dynamics of homogeneous two-channel TASEP with/without LK. In this chapter, we study thoroughly the impact of coupling strength on the dynamics of the model.

The terminology introduced in [16] has been adopted to recognize the different transition rates and the order of a transition rate is defined as below. The **order of a transition rate** Ω_r ; [$r = a, d, A, B$] is 10^{t-1} denoted by $O(\Omega_r)=10^{t-1}$ if it can be written as: $\Omega_r=s*10^{t-1}$; $s \in [1, 10]$, $t=0, 1, 2, 3$. Here, the value of r is depending upon the system size we are taking. The maximum value of Ω_r can be L and in our case we have chosen $L=1000$ so $r \leq 3$.

Now, we analyze the significant topological changes in the phase diagrams produced by higher order of lane-changing rate by keeping the order of other param-

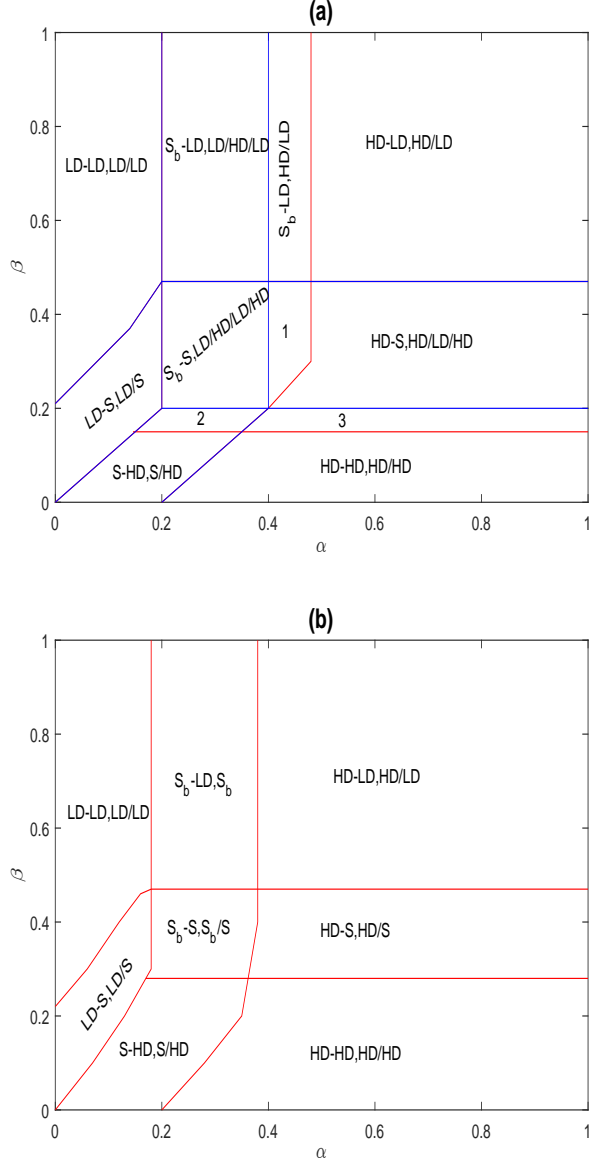


Figure 2.5: Phase diagram for $\Omega_d = 0.2$, $L = 1000$ with (a) $q = 0.25$, $\Omega_A = 60$, $\Omega_B = 30$. (b) $q = 0.25$, $\Omega_A = 600$, $\Omega_B = 300$, Notations:- 1: $(S_b-S, HD/LD/HD)$, 2: $(S_b-S, S/HD)$, 3: $(HD-S, HD/HD)$

eters such as attachment and detachment rates fixed to $O(\Omega_a) = O(\Omega_d) = 10^{-1}$.

For a weak bottleneck the effects of lane-changing rate on the phase diagram is of quantitative nature. We only observe some variations of small magnitudes in density profiles in both the lanes. So we will be focusing on the strong bottleneck to analyze the effect of coupling rate.

The major impact is seen for a strong bottleneck on increasing the order of lane-changing rates. We discuss the effect of Ω_A and Ω_B on phase diagram for $q = 0.25$. As we can see in fig.(2.5), there are no structural changes in the phase diagram until $O(\Omega_{A,B}) = 100O(\Omega_d)$, except some small translation of phase boundaries. So

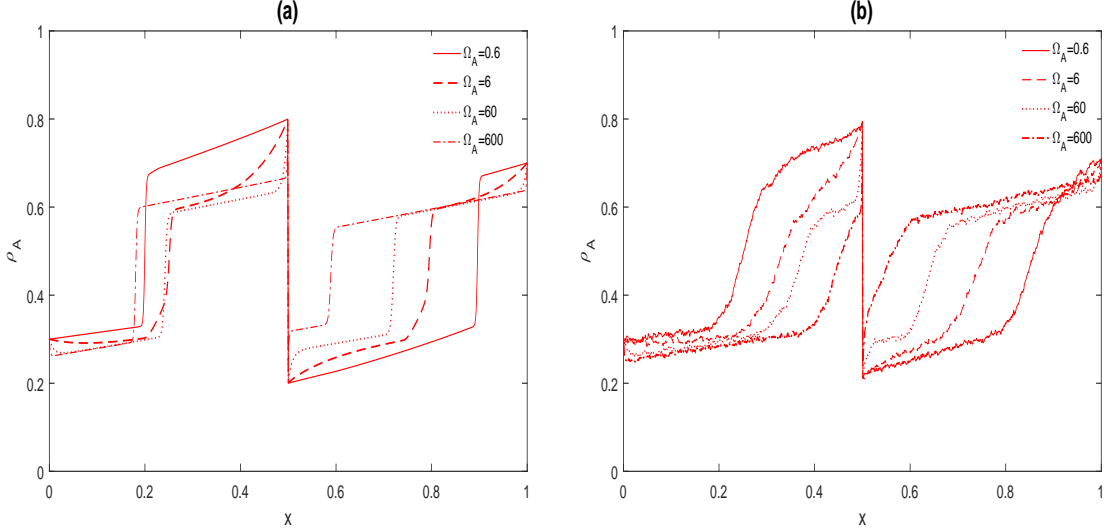


Figure 2.6: Variation in density profiles in lane A with respect to the order of lane-changing rates. Here, $\alpha=0.3$, $\beta=0.3$, $q=0.25$, (a)from CMF (b)from MCS

we skip the phase diagram for the case in which $O(\Omega_{A,B}) < 10$. The significant changes occur at $O(\Omega_{A,B}) \geq 10O(\Omega_d)$. When $O(\Omega_{A,B})=10O(\Omega_d)$, the effect of bottleneck on the density profiles in both the lanes reduces to the vicinity of the bottleneck(fig. 2.5(a)) . Note that, some of the phase boundaries have shifted. For example, the phases (S-HD,S/HD), (HD-HD,HD/HD) expand, whereas phase (S_b -S,S/HD) shrinks. Clearly, from fig.(2.5(a)) we can see that the phase (S_b -S,HD/HD) vanishes at this order of coupling rate. A further increase in the order to $O(\Omega_{A,B})=100O(\Omega_d)$ decreases the number of stationary phases and hence reduces the complexity of the phase diagram to a great extent. Observe that, there is a region in which bottleneck-induced shock occurs in lane B as well. The phase boundaries for both the lanes are coinciding with each other. So, the impact of strong bottleneck($q=0.25$) is now restricted to a comparatively smaller region in $\alpha - \beta$ plane. There are no subsequent changes in the phase diagram for $q=0.25$ on further increasing the lane-changing rates. This occurs due to the weakening of bottleneck effect by a rise in coupling-rate.

Fig.(2.6)(b), shows the phase transition in lane A on changing the order of lane-changing rates using Monte-Carlo simulations. Clearly, for $\alpha=0.3$, $\beta=0.3$ (S_b -S) phase is obtained in lane A. We find that the height of the jump at middle of the lane is same in all cases but shock's height is decreasing as we increase the order of coupling rates. In addition to it, the shock is moving leftwards.

2.3.3 Impact of system size

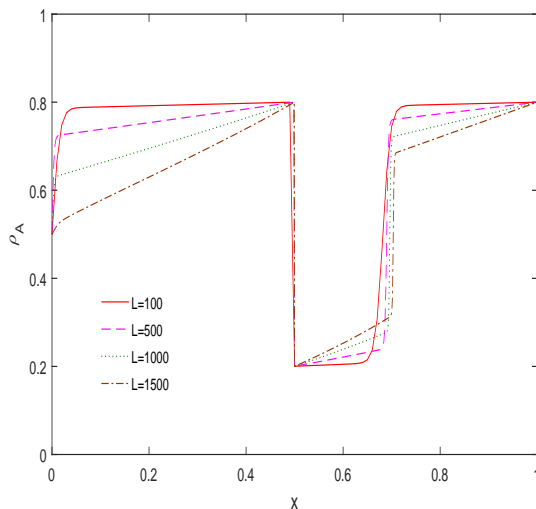


Figure 2.7: Variation in density profiles in lane A on changing the system size. Here, $\alpha=0.5$, $\beta=0.2$, $q=0.25$.

As shown in fig.(2.7), we can clearly note that there is not a huge transition with the increase in system size. The only change one observes is the sharpening of shock with respect to an increase in system size. Also, height of the shock in right subsystem of lane A is decreasing as we increase the length of the channel. Since there is no significant effect of L on the density profiles it is appropriate to analyze the steady state dynamics of $L=1000$.

2.4 Summary

In this chapter, we have studied a two-channel inhomogeneous TASEP with LK under partially asymmetric coupling conditions. The bottleneck is present in one of the lanes at a fixed position. The hybrid mean-field approach has been adopted along with Monte-Carlo simulations. Both the bottleneck rate and coupling strength are found to effect the system dynamics considerably. Significant non-equilibrium features such as boundary-induced phase transitions, bottleneck-induced spike and shock, mixed phases have been identified.

Chapter 3

Conclusions and Future Works

This chapter is the concluding part of the thesis and also proposes some suggestions towards which the present work can be further extended. Section 3.1 brings out the overall conclusions of the research work carried out in this thesis and in section 3.2 suggestions regarding the future research directions are provided.

3.1 Conclusion

In this thesis, an attempt has been made to provide a clear description of the role played by a single inhomogeneity in a two-channel totally asymmetric simple exclusion process with Langmuir Kinetics under asymmetric coupling situation. This is a novel work and has not been investigated so far in the literature. This model has suitable applicability to traffic flow and biological transport.

In our two-lane system bottleneck site is located at the middle of lane A , while lane B is kept homogeneous. Random sequential update rules have been used in our model. A generalized approach namely hybrid mean-field theory has been adopted to get the steady-state phase diagrams and density-profiles of the system. The effects of various parameters such as bottleneck rate, lane-changing rate and system size have been thoroughly investigated the important conclusions of the work done in this thesis are listed below.

- It has been seen that due to the partially asymmetric coupling there is a significant variation in the stationary phase diagrams. The complexity of phase diagram increases with the increase in bottleneck strength but at the complete blockage it reduces again.
- We have observed some important non-equilibrium features like bottleneck-induced shock, boundary-induced phase transitions, formation of spike and occurrence of mixed phases. Another important observation is the conversion of spike into bottleneck-induced shock.
- Regarding the impact of coupling strength one can conclude that higher order of lane-changing rates weakens the bottleneck effect.

- Also, no finite size effect has been observed on studying the impact of system size on the steady-state dynamics.

3.2 Scope for future work

Research is an iterative and continuous procedure. With this statement we can say that the present model studied in this thesis can be further analyzed more deeply. One can also study the effects of attachment and detachment rates on the steady-state dynamics of the system. Role of binding constant and shock dynamics can be further explored. The outcomes of present thesis can be helpful in traffic networks which are widely prevailing in real world. It might be insightful towards the networking of roads or highways in a city. Efficient modifications can be done in our model to explore cytoskeletal filaments which form a complex network inside the cell.

References

- [1] C. T. MacDonald, J. H. Gibbs, and A. C. Pipkin, “Kinetics of biopolymerization on nucleic acid templates,” *Biopolymers*, vol. 6, no. 1, pp. 1–25, 1968.
- [2] D. Chowdhury, L. Santen, and A. Schadschneider, “Statistical physics of vehicular traffic and some related systems,” *Physics Reports*, vol. 329, no. 4, pp. 199–329, 2000.
- [3] S. Klumpp and R. Lipowsky, “Traffic of molecular motors through tube-like compartments,” *Journal of Statistical Physics*, vol. 113, no. 1, pp. 233–268, 2003.
- [4] J. Howard *et al.*, “Mechanics of motor proteins and the cytoskeleton,” 2001.
- [5] T. Chou and G. Lakatos, “Clustered bottlenecks in mrna translation and protein synthesis,” *Physical review letters*, vol. 93, no. 19, p. 198101, 2004.
- [6] K. Nagel, “Particle hopping models and traffic flow theory,” *Phys. Rev. E*, vol. 53, pp. 4655–4672, May 1996.
- [7] N. Rajewsky, L. Santen, A. Schadschneider, and M. Schreckenberg, “The asymmetric exclusion process: Comparison of update procedures,” *Journal of statistical physics*, vol. 92, no. 1, pp. 151–194, 1998.
- [8] B. Derrida, “An exactly soluble non-equilibrium system: the asymmetric simple exclusion process,” *Physics Reports*, vol. 301, no. 1, pp. 65–83, 1998.
- [9] J. Krug, “Boundary-induced phase transitions in driven diffusive systems,” *Physical review letters*, vol. 67, no. 14, p. 1882, 1991.
- [10] E. Pronina and A. B. Kolomeisky, “Two-channel totally asymmetric simple exclusion processes,” *Journal of Physics A: Mathematical and General*, vol. 37, no. 42, p. 9907, 2004.
- [11] E. Pronina and A. B. Kolomeisky, “Asymmetric coupling in two-channel simple exclusion processes,” *Physica A: Statistical Mechanics and its Applications*, vol. 372, no. 1, pp. 12–21, 2006.
- [12] K. Tsekouras and A. Kolomeisky, “Parallel coupling of symmetric and asymmetric exclusion processes,” *Journal of Physics A: Mathematical and Theoretical*, vol. 41, no. 46, p. 465001, 2008.
- [13] M. Evans, Y. Kafri, K. Sugden, and J. Tailleur, “Phase diagrams of two-lane driven diffusive systems,” *Journal of Statistical Mechanics: Theory and Experiment*, vol. 2011, no. 06, p. P06009, 2011.
- [14] A. Parmeggiani, T. Franosch, and E. Frey, “Totally asymmetric simple exclusion process with langmuir kinetics,” *Physical Review E*, vol. 70, no. 4,

- p. 046101, 2004.
- [15] N. Mirin and A. B. Kolomeisky, “Effect of detachments in asymmetric simple exclusion processes,” *Journal of statistical physics*, vol. 110, no. 3, pp. 811–823, 2003.
 - [16] I. Dhiman and A. K. Gupta, “Effect of coupling strength on a two-lane partially asymmetric coupled totally asymmetric simple exclusion process with langmuir kinetics,” *Physical Review E*, vol. 90, no. 1, p. 012114, 2014.
 - [17] A. K. Gupta and I. Dhiman, “Asymmetric coupling in two-lane simple exclusion processes with langmuir kinetics: Phase diagrams and boundary layers,” *Physical Review E*, vol. 89, no. 2, p. 022131, 2014.
 - [18] R. Jiang, R. Wang, and Q.-S. Wu, “Two-lane totally asymmetric exclusion processes with particle creation and annihilation,” *Physica A: Statistical Mechanics and its Applications*, vol. 375, no. 1, pp. 247–256, 2007.
 - [19] R. Wang, R. Jiang, M. Liu, J. Liu, and Q.-S. Wu, “Effects of langmuir kinetics on two-lane totally asymmetric exclusion processes of molecular motor traffic,” *International Journal of Modern Physics C*, vol. 18, no. 09, pp. 1483–1496, 2007.
 - [20] P. Pierobon, M. Mabilia, R. Kouyos, and E. Frey, “Bottleneck-induced transitions in a minimal model for intracellular transport,” *Physical Review E*, vol. 74, no. 3, p. 031906, 2006.
 - [21] J. Dong, B. Schmittmann, and R. Zia, “Towards a model for protein production rates,” *Journal of Statistical Physics*, vol. 128, 2007.
 - [22] P. Greulich and A. Schadschneider, “Phase diagram and edge effects in the asep with bottlenecks,” *Physica A: Statistical Mechanics and its Applications*, vol. 387, no. 8, pp. 1972–1986, 2008.
 - [23] S. A. Janowsky and J. L. Lebowitz, “Exact results for the asymmetric simple exclusion process with a blockage,” *Journal of Statistical Physics*, vol. 77, no. 1, pp. 35–51, 1994.
 - [24] S. A. Janowsky and J. L. Lebowitz, “Finite-size effects and shock fluctuations in the asymmetric simple-exclusion process,” *Physical Review A*, vol. 45, no. 2, p. 618, 1992.
 - [25] A. B. Kolomeisky, “Asymmetric simple exclusion model with local inhomogeneity,” *Journal of Physics A: Mathematical and General*, vol. 31, no. 4, p. 1153, 1998.
 - [26] K. Qiu, X. Yang, W. Zhang, D. Sun, and Y. Zhao, “Density profiles in the totally asymmetric exclusion processes with both local inhomogeneity and langmuir kinetics,” *Physica A: Statistical Mechanics and its Applications*, vol. 373, pp. 1–10, 2007.

- [27] Q.-H. Shi, R. Jiang, M.-B. Hu, and Q.-S. Wu, “Strong asymmetric coupling of two parallel exclusion processes,” *Journal of Statistical Physics*, vol. 142, no. 3, pp. 616–626, 2011.
- [28] R. Wang, M. Liu, and R. Jiang, “Local inhomogeneity in two-lane asymmetric simple exclusion processes coupled with langmuir kinetics,” *Physica A: Statistical Mechanics and its Applications*, vol. 387, no. 2, pp. 457–466, 2008.
- [29] I. Dhiman and A. K. Gupta, “Collective dynamics of an inhomogeneous two-channel exclusion process: Theory and monte carlo simulations,” *Journal of Computational Physics*, vol. 309, pp. 227–240, 2016.